Probing the Ultimate Limits of Plasmonic Enhancement

C. Ciracì,[1]* R. T. Hill,[2] J. J. Mock,[1] Y. Urzhumov,[1] A. I. Fernández-Domínguez,[3] S. A. Maier,[3] J. B. Pendry,[3] A. Chilkoti,[2,4] D. R. Smith[1]

Metals support surface plasmons at optical wavelengths and have the ability to localize light to subwavelength regions. The field enhancements that occur in these regions set the ultimate limitations on a wide range of nonlinear and quantum optical phenomena. We found that the dominant limiting factor is not the resistive loss of the metal, but rather the intrinsic nonlocality of its dielectric response. A semiclassical model of the electronic response of a metal places strict bounds on the ultimate field enhancement. To demonstrate the accuracy of this model, we studied optical scattering from gold nanoparticles spaced a few angstroms from a gold film. The bounds derived from the models and experiments impose limitations on all nanophotonic systems.

One of the most remarkable phenomena associated with metals at optical wavelengths is field enhancement. Local optical fields within a metal nanostructure can achieve strengths that are orders of magnitude greater than that of the incident field. This singular feature of metals serves as the fundamental mechanism for a host of radiative and scattering processes associated with nanophotonic systems. Field enhancement has been shown to affect surface-enhanced Raman scattering (*1*); nonlinear processes, such as enhanced harmonic generation (*2*) or wave mixing (*3*); nanolasing (*4*); plasmonic sensing (*5*); and enhancement of spontaneous emission (*6*).

The largest field enhancements in nanoplasmonic systems occur near sharp asperities or corners associated with metal nanoparticles (NPs) and within the subnanometer gaps formed between NP aggregates. An incident optical field drives currents across the NP, resulting in peak currents flowing through the NP during one part of the cycle, and a peak surface charge density during the other part of the cycle. Using the conventional, classical description of the metal's response—or local model—at the moment of peak polarization, the charges can be considered crushed into a layer of infinitesimal thickness along the NP surface, resulting in the standard surface charge density picture. Structures that possess a singularity, such as spheres that touch at a point, have been shown to possess continuous scattering spectra associated with compression of the surface plasmon wave field at the singularity. According to the local model, a pulse of surface plasmons launched into such a system would travel toward but never reach the singularity, giving rise to energy compression and enormous field enhancements (*7*).

It would appear, then, that virtually unbounded field enhancements should be possible if well-defined subnanometer gaps can be created between nanostructures with sufficiently smooth surfaces. However, in a real metal, polarization charge densities are not perfectly localized at a surface but are slightly spread over a thickness near the boundary. This dispersion of the charge effectively smoothes the singularities: Charges no longer reside exactly at the surface, but acquire some volume as the charge density spreads into the NP. The scattering spectrum ceases to be continuous and is now discrete, with correspondingly reduced field enhancements (*8*, *9*). These effects have long been recognized by theorists; for example, Fuchs and Claro (*10*) showed that the nonlocal effects considered here limit the response of almost-touching spheres.

The local model for free electron response inside metallic structures is insufficient to describe metals whose critical dimensions are on the order of a few nanometers or less. A more appropriate description should take into account atomic and subatomic interactions, and electron-electron repulsion in particular. The Pauli exclusion principle forbids two fermions from occupying the same quantum state at a given time, resulting in a repulsive force between charge carriers. Along with the classical Coulomb force, the quantum repulsion manifests itself as a pressure in an electron gas that resists the compression induced by an applied electromagnetic field. This electron pressure may be taken into account by a hydrodynamic description of the collective motion of the electrons inside a metal (*11*). The currents **J** inside a metal induced by an electric field **E** oscillating at frequency ω can be described by the following equation (*12*):

$$\beta^2\nabla(\nabla\cdot\mathbf{J}) + (\omega^2 + i\gamma\omega)\mathbf{J} = i\omega\omega_p^2\varepsilon_0\mathbf{E} \quad (1)$$

where ε_0 is the vacuum permittivity, and γ and ω_p are the damping coefficient and the plasma frequency, respectively, which also appear in the conventional Drude formula, $\varepsilon(\omega) = 1 - [\omega_p^2/(\omega^2 + i\gamma\omega)]$, and β—approximately the speed of sound in the Fermi-degenerate plasma of conduction electrons (*11*)—is proportional to the Fermi velocity v_F.

The effect of including the pressure term in the electron response is that the longitudinal dielectric function, ε_L, becomes nonlocal, depending on the propagation vector **k** in addition to the frequency, as follows:

$$\varepsilon_L(\mathbf{k},\omega) = 1 - \frac{\omega_p^2}{\omega^2 + i\gamma\omega - \beta^2|\mathbf{k}|^2} \quad (2)$$

whereas the transverse response is unchanged.

The simple picture, then, of a surface charge layer with infinitesimal extent must be replaced with a continuous charge density, whose extent will be determined by $\beta/\omega_p \propto \lambda_{TF}$, where $\lambda_{TF} = v_F/\omega_p$ is the Thomas-Fermi screening length. Rather than a strict surface charge density, the nonlocality produces a volume charge density that spreads out from the surface a distance ~λ_{TF} on the order of 1 Å. As a result, the real behavior

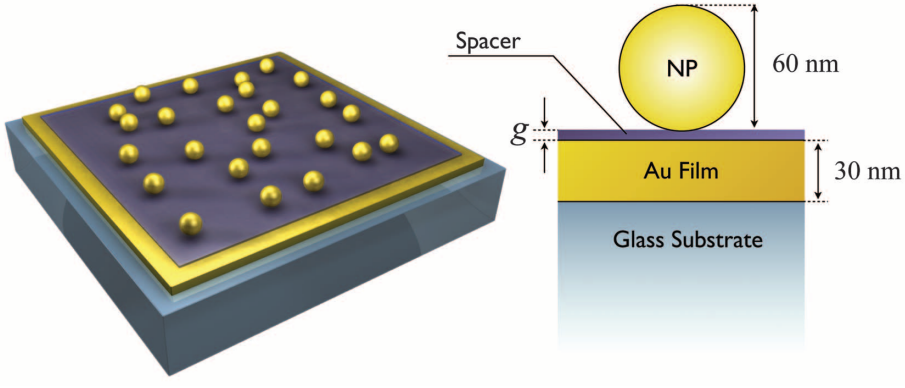

Fig. 1. Geometry of the film-coupled nanoparticle. (**Left**) Schematic of the sample. (**Right**) Cross section of a single film-coupled nanosphere.

[1]Center for Metamaterials and Integrated Plasmonics and Department of Electrical and Computer Engineering, Duke University, Durham, NC 27708, USA. [2]Center for Biologically Inspired Materials and Material Systems, Duke University, Durham, NC 27708, USA. [3]Department of Physics, Blackett Laboratory, Imperial College London, London SW7 2AZ, UK. [4]Department of Biomedical Engineering, Duke University, Durham, NC 27708, USA.

*To whom correspondence should be addressed. E-mail: cristian.ciraci@duke.edu

of the optical characteristics of subnanometer-length systems may deviate from local model predictions (*13*).

A full quantum treatment of optical response is possible only for very small spheres. Therefore, it is critical to develop and verify a semi-empirical model that can be applied to spheres of dimensions greater than a few nanometers. Here, we use the hydrodynamic model to take quantum effects into account, assuming that delocalization of surface charge is the dominant process. Alternative semi-empirical models have been developed that emphasize the tunneling current between two surfaces, which is present at very small separations (*14*–*16*). We find that for the geometrical parameters of our experiments, the hydrodynamic model gives an excellent account of our data, although we concede that tunneling current may well play an important role for smaller dimensions.

To date, the experimental study of nonlocality on coupled plasmonic systems has been hampered by the difficulty in achieving reliable and precise control of subnanometer interparticle spacing. Even a relatively simple system, such as two nanospheres separated by a subnanometer gap, remains a challenge for colloidal or lithographic synthesis methods. By contrast, one closely related system—a metal nanosphere positioned a specified distance above a metallic film—is simple to fabricate and provides exquisite control of the spacing. The film-coupled nanosphere geometry (Fig. 1) involves the deposition of a metal film by standard sputtering or evaporation methodologies, followed by solution deposition of a molecular dielectric layer and chemisorption of chemically synthesized metal NPs on the spacer layer.

As the NPs are brought closer to the film, the coupling between a given NP and its virtual image induces a red shift in the peak of the plasmon resonance wavelength, which can be detected as the peak intensity in the measured scattering cross section. Because the spacer layer exhibits tremendous uniformity, the scattering behavior of the NPs is remarkably uniform, and scattering measurements on a slide sample from ensembles of NPs are representative of the typical scattering of an individual film-coupled NP, as confirmed by dark-field microscopy. Numerical simulations reveal the expected behavior of strongly localized fields between the NP and film, related to the interaction of the NP with its electromagnetic image (Fig. 2). In addition, the field very near the surface of the metal sphere decays exponentially away from the surface on a scale given essentially by λ_{TF}.

The plasmon resonant scattering peak positions and enhancement factor for gap dimensions between 0.1 nm and 10 nm can be calculated using both the local model and the nonlocal model (Fig. 3). The plasmon resonance of the NP shifts predictably toward the red, and the field enhancement grows as the gap dimension decreases. If the local model for the metal dielectric function is used, the expected shift in

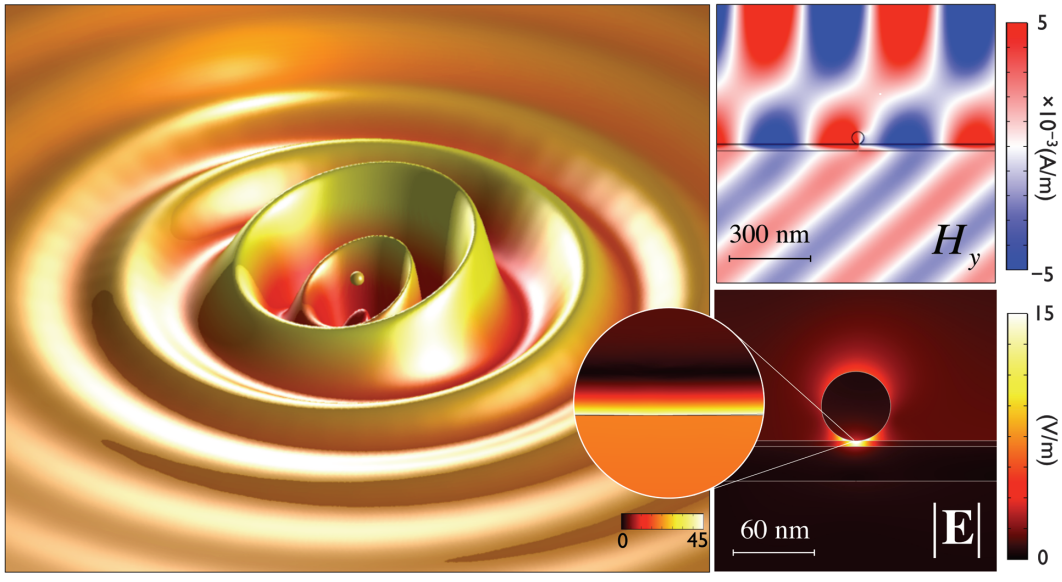

Fig. 2. Simulation of a single film-coupled nanoparticle. (**Left**) Relative electron surface density showing the excited surface plasmon polariton propagating over the metal film. The nanoparticle can be seen at the center. (**Upper right**) A plane wave is incident at 75° from normal on the nanoparticle. (**Lower right**) A close-up of the near fields surrounding the nanosphere; note the large field amplitude directly below the sphere. Looking closer yet, it can be seen that the fields penetrate into the nanosphere by a distance on the order of the Thomas-Fermi screening length.

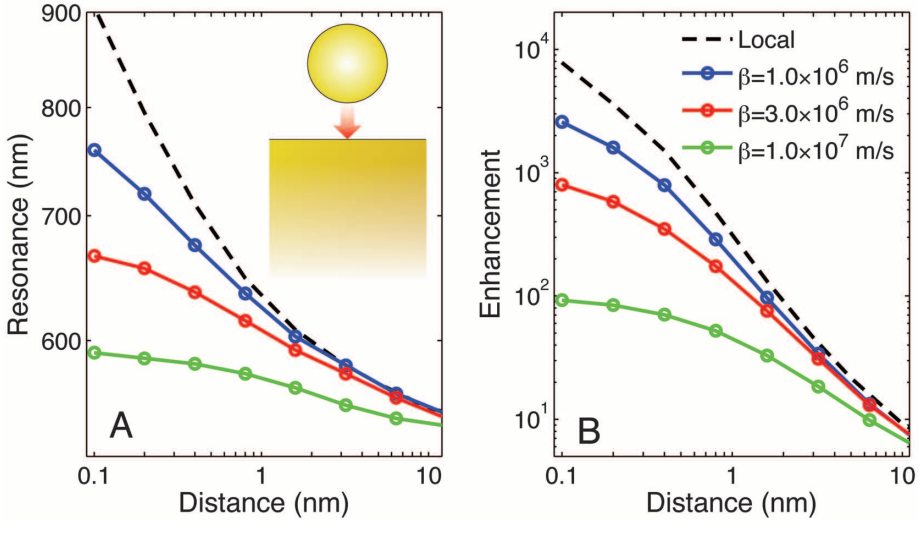

Fig. 3. Behavior of the film-coupled nanosphere, assuming a local model and the nonlocal model with various values of β, as a function of separation distance. Calculations refer to a gold nanosphere of radius r = 30 nm on a film 300 nm thick. (**A**) Position of the peak scattering intensity as a function of gap size. (**B**) The corresponding field enhancement ratio. Note that in the absence of nonlocal effects, the peak scattering wavelength is extreme and the field enhancement grows to enormous values; nonlocality places a limit on the ultimate enhancement.

the plasmon resonance wavelength is pushed to nearly $\lambda = 900$ nm, corresponding to a peak local field enhancement of ~10^4 (Fig. 3). The presence of a nonzero β considerably modifies the plasmon resonance wavelength shift for separation distances below 5 nm. From 1 nm to 0.1 nm, the impact of the nonlocal electronic response is decisive, causing the peak resonance wavelength to occur at values much lower than that predicted by the local model. For the realistic value of the nonlocal parameter, $\beta = 1.0 \times 10^6$ m/s—as expected from prior measurements and theory—the peak resonance wavelength shift is capped near 750 nm, a full 150-nm difference from that predicted using the local model.

The impact of spreading the charge thus leads to substantial optical shifts that are easily measurable by spectroscopic techniques. The field enhancement is still extremely large relative to the analogous 2D system (*7*), even with the nonlocal interactions taken into account. The expected enhancement exceeds values of 10^3 for realistic values of the parameter β (Fig. 3B). Far more than material losses, the nonlocality plays the dominant role in limiting electromagnetic enhancement of NPs, reducing the dimer or film-coupled NP peak enhancement by a factor of ~4.

An experimental test of the validity of our predictions requires precise control over extremely short gap lengths. We deposit spacer layers using either layer-by-layer (LBL) deposition of polyelectrolytes (*5*, *17*, *18*), for separations that range from 2.8 to 26.6 nm, or by the formation of self-assembled monolayers (SAMs) of amine-terminated alkanethiols for even smaller separation distances that range from 0.5 to 2.0 nm. We first prepare a set of gold films 30 nm thick, then incubate the gold films with either a series of polyelectrolytes or a set of amine-terminated alkanethiols wherein the gap length is tuned by the number of carbon atoms in the chain (Fig. 4A). The thicknesses of the SAM spacer layers have been estimated using a theoretical approach (*12*), as standard ellipsometry measurements have been shown to produce systematically low thickness values for such thin SAMs on gold surfaces (*19*).

The optical response of the NPs deposited on the spacer layers is measured by illuminating the sample with white light and collecting the scattered light through a dark-field objective. The collected light is then directed through an image plane aperture (diameter 1 mm) to the spectrometer. The plasmon resonant scattering spectra for each of the samples—which correspond to different gap sizes as determined by the chain length of the SAM—are shown in Fig. 4C. The results of both the local and nonlocal model simulations are plotted alongside the collected data in Fig. 4D, showing the plasmon resonance peak position dependence on film-NP separation distance. We found that the electric permittivity of the spacer layer must be taken into account in the models to achieve the best fit. We used a nondispersive index of refraction of $n = 1.8$. Comparison of the numerical simulations to our experimental results (Fig. 4D) reveals that the nonlocal model is in excellent agreement with the experimentally measured scattering peaks, confirming that the actual dielectric function is modified by the electron pressure term.

The agreement obtained demonstrates that the hydrodynamic model is a powerful tool that incorporates quantum effects in macroscopic systems, and shows that in certain cases the impact of nonlocality may prevail over purely quantum effects such as electron tunneling. Although direct measurements of near-field enhancement remain difficult at such scales, our results provide strong experimental support in setting an upper limit to the maximum field enhancement achievable with plasmonic systems.

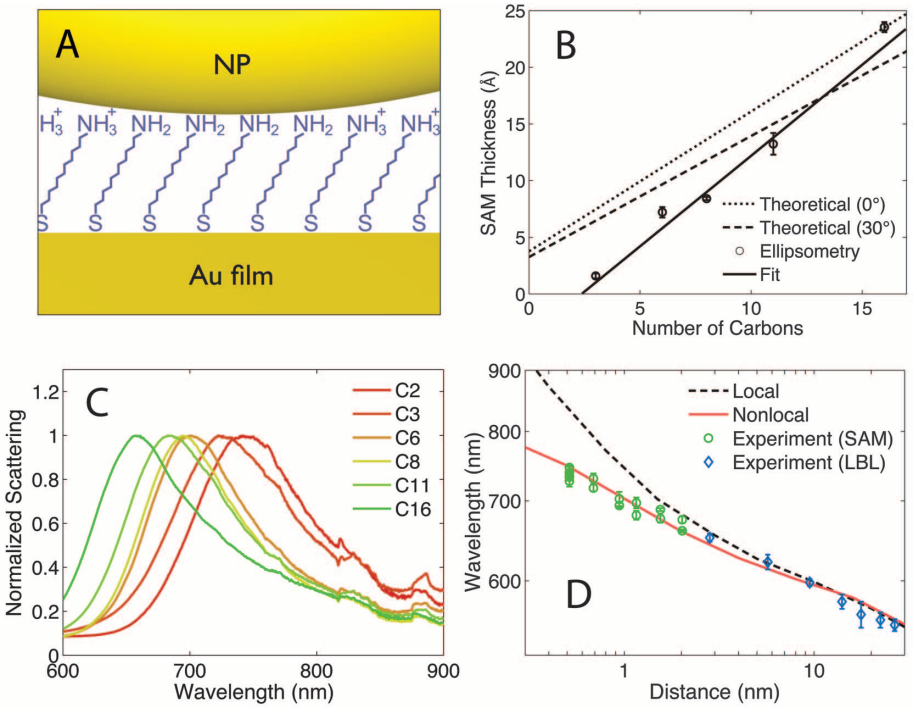

Fig. 4. Experimental confirmation of nonlocal contributions to surface plasmon scattering. (**A**) Schematic of nanoparticle-film gap system showing a gold nanoparticle separated from the film by an amine-terminated alkanethiol SAM. (**B**) Thickness of the SAM layers as a function of the number of carbon atoms. (**C**) Normalized dark-field measured spectra of ensembles of film-coupled nanoparticles for SAM spacer layers of different numbers of carbon atoms. (**D**) Comparison of experimental measurements from SAM- and LBL-type spacers with numerical results with $\beta = 1.27 \times 10^6$ m/s.

References and Notes

1. M. Moskovits, *Rev. Mod. Phys.* **57**, 783 (1985).
2. M. Scalora *et al.*, *Phys. Rev. A* **82**, 043828 (2010).
3. J. Renger, R. Quidant, N. van Hulst, L. Novotny, *Phys. Rev. Lett.* **104**, 046803 (2010).
4. R. F. Oulton *et al.*, *Nature* **461**, 629 (2009).
5. J. J. Mock, R. T. Hill, Y.-J. Tsai, A. Chilkoti, D. R. Smith, *Nano Lett.* **12**, 1757 (2012).
6. Y. Gu *et al.*, *Nano Lett.* **12**, 2488 (2012).
7. A. I. Fernández-Domínguez, S. A. Maier, J. B. Pendry, *Phys. Rev. Lett.* **105**, 266807 (2010).
8. A. I. Fernández-Domínguez, A. Wiener, F. J. García-Vidal, S. A. Maier, J. B. Pendry, *Phys. Rev. Lett.* **108**, 106802 (2012).
9. C. David, F. J. García de Abajo, *J. Phys. Chem. C* **115**, 19470 (2011).
10. R. Fuchs, F. Claro, *Phys. Rev. B* **35**, 3722 (1987).
11. A. D. Boardman, *Electromagnetic Surface Modes* (Wiley, New York, 1982).
12. See supplementary materials on *Science* Online.
13. G. Toscano, S. Raza, A.-P. Jauho, N. A. Mortensen, M. Wubs, *Opt. Express* **20**, 4176 (2012).
14. J. Zuloaga, E. Prodan, P. Nordlander, *Nano Lett.* **9**, 887 (2009).
15. D. C. Marinica, A. K. Kazansky, P. Nordlander, J. Aizpurua, A. G. Borisov, *Nano Lett.* **12**, 1333 (2012).
16. R. Esteban, A. G. Borisov, P. Nordlander, J. Aizpurua, *Nature Commun.* **3**, 825 (2012).
17. R. T. Hill *et al.*, *Nano Lett.* **10**, 4150 (2010).
18. G. Decher, *Science* **277**, 1232 (1997).
19. C. Bain *et al.*, *J. Am. Chem. Soc.* **111**, 321 (1989).

Acknowledgments: We thank M. Scalora, S. Wolter, and A. Moreau for helpful input and discussion. Supported by Air Force Office of Scientific Research grant FA9550-09-1-0562 and by the Army Research Office through Multidisciplinary University Research Initiative grant W911NF-09-1-0539. Also supported by the Leverhulme Trust and the Marie Curie Actions (J.B.P., S.A.M., and A.I.F.-D.), NIH grant R21EB009862 (A.C.), and NIH F32 award F32EB009299 (R.T.H.).

Supplementary Materials

www.sciencemag.org/cgi/content/full/337/6098/1072/DC1
Materials and Methods
Supplementary Text
Figs. S1 and S2
References (*20*–*25*)

17 May 2012; accepted 18 July 2012
10.1126/science.1224823